AGU PUBLICATIONS

Global Biogeochemical Cycles

Supporting Information for

Suppression of nitrogen deposition on global forest soil CH_4 uptake depends on nitrogen status

Xiaoyu Cen[1,2,3], Nianpeng He[1,4,5*], Mingxu Li[1,6], Li Xu[1,2], Xueying Yu[3], Weixiang Cai[7], Xin Li[1,2], Klaus Butterbach-Bahl[8,9]

[1] Key Laboratory of Ecosystem Network Observation and Modeling, Institute of Geographic Sciences and Natural Resources Research, Chinese Academy of Sciences, Beijing 100101, China

[2] College of Resources and Environment, University of Chinese Academy of Sciences, Beijing 100049, China

[3] Department of Earth System Science, Stanford University, Stanford, CA 94305, USA

[4] Key Laboratory of Sustainable Forest Ecosystem Management-Ministry of Education, Northeast Forestry University, Harbin, 150040, China

[5] Northeast Asia ecosystem Carbon Sink Research Center, Northeast Forestry University, Harbin, 150040, China

[6] Earth Critical Zone and Flux Research Station of Xing'an Mountains, Chinese Academy of Sciences, Daxing'anling 165200, China

[7] School of Ecology and Nature Conservation, Beijing Forestry University, Beijing 100083, China

[8] Department of Agroecology, Pioneer Center Land-CRAFT, Aarhus University, 8000 Aarhus C, Denmark

[9] Institute for Meteorology and Climate Research, Atmospheric Environmental Research, Karlsruhe Institute of Technology, 82467 Garmisch- Partenkirchen, Germany

Contents of this file

Text S1 to S2
Figures S1 to S9
Tables S1 to S4

Additional Supporting Information (Files uploaded separately)

Captions for Data Sets S1 to S9
Captions for Code S1

Introduction

The uploaded Data Set S1 (CH_4_exp dataset in main text) was used to derive the response factors of soil CH_4 flux to N input in global forests; Data Set S2 (CH_4_obs dataset in main text) was used to estimate the soil CH_4 fluxes in global forests; Data Sets S3–S7 were used to classify the N-limited and N-saturated forests on global level; Data Set S8 contains environmental factors (MAT, MAP, soil texture, etc.) for global estimations; Data Set S9 contains global forest soil CH_4 budgets reported in previous studies. The data analysis process and produced figures can be replicated with the uploaded R script (Code S1).

Text S1. Nitrogen saturation status of global forests indicated by sensitivity of soil N_2O emission to N deposition.

Globally, human-induced increase in atmospheric N deposition is changing forests from a nitrogen-limited to nitrogen-saturated status. In N-limited forests, plants and microbes utilize N conservatively for a lower proportion of input N to be leaked from tight N cycling processes (Chapman et al., 2006; Van Der Heijden et al., 2008). However, when forests become N-saturated, input N exceeds the N demand of plants and microbes, leading to excessive utilization of N, and thus, the N cycle becomes more open (Hietz et al., 2011). Therefore, a higher proportion of input N is lost via leaching or gaseous emission (Aber et al., 1989). This implies that increased gaseous N emissions (N_2O, NO, and N_2) per unit of N deposition (i.e., higher sensitivity of gaseous N emissions to N deposition) may indicate forests reaching N saturation (Aber et al., 1998). Coincidently, studies have measured nitrous oxide (N_2O) greenhouse gas emissions under different N input levels since the 1980s in global forests, using a controlled experiment design and standard sampling method (Holland et al., 1999). The accumulated experimental data provide an opportunity to quantify the sensitivity of N_2O emissions to N deposition in various forests, and indicate the N limitation or saturation status of global forests.

Gathering data

To quantify the sensitivity of soil N_2O emissions to N deposition (s_N), we compiled soil N_2O emission data observed in N addition experiments conducted in global forests. On 03/30/2022, we searched for papers and theses published before 01/01/2022 from the Web of Science Core Collection database (www.webofscience.com) and China National Knowledge Infrastructure Theses and Dissertations Database (https://oversea.cnki.net/kns?dbcode=CDMD), using the following keywords: “forest” AND “greenhouse gas” OR “N_2O” OR “nitrous oxide”. The retrieved 7422 papers and 718 theses were then refined manually based on the following criteria: (i) experimental N addition was conducted in forest ecosystem; (ii) literature recorded the location, time, and dose of the experiment(s); (iii) soil N_2O flux was observed in experimental sites and measured using gas chromatograph technique (Holland et al., 1999). As a result, the compiled “N_2O_exp” dataset (Data Set S3) contained 553 observations from 102 sites worldwide (Fig. S7).

Similarly, we compiled data on the soil N_2O emission rates of global forests observed under natural conditions. We refined from the same papers and theses as above, using a different set of criteria: (i) no nutrients, including N, were artificially added to the forest site so the site only received naturally deposited N; (ii) literature recorded the location, and time of flux measurement; (iii) soil N_2O flux was observed in the field and measured using gas chromatograph technique (Holland et al., 1999). The compiled “N_2O_obs” dataset (Data Set S4) contained 246 observations from 140 sites worldwide (Fig. S7).

In addition, we compiled data on total N loss (N leaching and gaseous N emission combined), N leaching, and change in soil N pool, from N addition experiments in global forests. We searched in the aforementioned databases using the following keywords: “forest” AND “nitrogen addition” OR “fert*” AND “nitrogen loss” OR “nitrogen leaching” OR “nitrogen budget”. Retrieved 2693 papers and theses were then refined based on the following criteria: (i) literature recorded the location, time, and dose of experimental N addition in forests; (ii) total N loss rate, N leaching rate, or change rate of soil N pool was observed or estimated in the experiments. The compiled “Ncycle_exp” dataset (Data Set S5) contained 169 observations from 37 sites (Fig. S7).

To analyze the relationship between s_N and N saturation status, we compiled data on field-observed N-limited and N-saturated forests indicated by N leaching. On 10/31/2022, we searched for literature in the aforementioned databases using the following keywords: “forest” AND “leaching” AND “nitrogen limit*” OR “nitrogen saturat*”. Retrieved 823 papers and theses were then refined based on the following criteria: (i) literature recorded whether the forest was N-limited or N-saturated, and its location; (ii) literature used nitrogen leaching as an indicator of N limitation or saturation status. The compiled “Nleach” dataset (Data Set S6) contains 136 observations from 92 sites worldwide (Fig. S6). We also used data on field-observed N-limited and N-saturated ecosystems indicated by plant growth response to N input (“NuLi” dataset; Data Set S7) from a published database by Du et al. (2020). It covers 106 sites worldwide, 65 of which are forest sites (Fig. S6).

Moreover, we extracted auxiliary information from the literature on environmental factors (including mean annual temperature, MAT; mean annual precipitation, MAP; mean annual N deposition rate, N_{depo}; coefficients of temporal variation, MAT.cv, MAP.cv, and N_{depo}.cv; soil sand content, soil clay content, and other soil properties) for the forest sites in the datasets. However, the literature did not provide the necessary auxiliary information for all sites; therefore, spatial datasets were used to fill in the missing data based on the location of the sites. Global temperature and precipitation datasets were obtained from the Climatic Research Unit, University of East Anglia (https://crudata.uea.ac.uk/cru/data/hrg/cru_ts_4.03/). The soil C:N ratio was obtained from a published database(Shangguan et al., 2014). Other soil properties were obtained from the HWSD dataset (https://www.fao.org/soils-portal/data-hub/soil-maps-and-databases/harmonized-world-soil-database-v12/en/). N deposition rate and forest cover data were from published databases (Ackerman et al., 2019; Liu et al., 2020). The forest biome map was derived from the Global Forest Monitoring project (Hansen et al., 2010).

Quantifying the sensitivity of soil N_2O emissions to N deposition

Under low N input, the soil N_2O emission rate responds almost linearly to N input, whereas high N input may induce non-linear responses (Aber et al., 1998; D.-G. Kim et al., 2013). High N input may change ecosystem properties, leading to a deviation from the natural response of ecosystems to environmental change. Therefore, we used a linear model (Eq. S1) to define and quantify the sensitivity (s_N) of soil N_2O emissions to N deposition (or low N input), for s_N to reflect ecosystem properties (i.e., N saturation status).

$$R_{N2O} = s_N \times N_{depo} + R_0 \quad \text{(Eq. S1)}$$

where R_{N2O} is the soil N_2O emission rate (kgN_2O-N ha^{-1} yr^{-1}), N_{depo} is the atmospheric N deposition rate (kg N ha^{-1} yr^{-1}), s_N is the sensitivity of soil N_2O emission to N deposition, quantified as soil N_2O emission per unit of low N input (kgN_2O-N kgN^{-1}), and R_0 is the background soil N_2O emission rate when there is no N deposition or artificial N addition (kgN_2O-N ha^{-1} yr^{-1}).

A segmented regression analysis on N_2O_exp dataset showed that there is one change point in the linear relationship between N input rate and R_{N2O}, which is 174.70 ± 19.73 kgN ha^{-1} yr^{-1}. That is in line with change points estimated or used in previous studies (Bouwman et al., 2002; Hoben et al., 2011; M. Lu et al., 2022; McSwiney & Robertson, 2005; Shcherbak et al., 2014). Conservatively, experimental data with N addition rates not exceeding 150 kg N ha^{-1} yr^{-1} were used as "low N input" data in further analysis. The N deposition rates in global forests were lower than the level (Ackerman et al., 2019). For all the low-N input data in the N_2O_exp dataset, we aggregated them to 0.5° × 0.5° grids based on their coordinates to match the spatial resolution with environmental factors and reduce random errors in sampling. A linear model (Model: R_{N2O} ~ N input rate) was built for each grid with low-N input data. The slope of the linear model was the estimated s_N of the grid (Table S3).

Based on the estimated s_N of all grids and the corresponding environmental factors, we built a generalized linear model to simulate s_N (Table S4). In addition, another generalized linear model was built to simulate R_0.

To validate s_N, we firstly used the modeled s_N, together with the modeled R_0 and N_{depo} datasets, to estimate R_{N2O} (Eq. S1). The estimated R_{N2O} values were compared with R_{N2O} observations (N_2O_obs dataset) and indirectly validated the intermediate variable s_N (Fig. S8). In addition, s_N was validated using a second approach. The sensitivity of N loss to N input (c_1), the sensitivity of N leaching to N input (c_2), and the end-product ratio of nitrification and denitrification processes (c_3) were either derived from the Ncycle_exp dataset or extracted from the literature; s_N was then calculated from these parameters (Eq. S2).

$$s_N = c_3 \times (c_1 - c_2) \qquad \text{(Eq. S2)}$$

The limited observations allowed us to calculate s_N on a biome scale (Fig. S7), which was then compared with the biome-mean value of the modeled s_N to validate it. The good agreement also validated the modeled s_N (r = 0.998).

Determining N saturation status of global forests using s_N

We tested whether s_N can distinguish between N-limited and N-saturated forests using data from forests having field-observed N saturation status data. First, we combined Nleach and NuLi datasets to enlarge the sample size and derive a universal classification. Excluding three duplicate sites in both datasets, the combined dataset had 154 sites with field-observed N saturation status (86 N-limited and 68 N-saturated sites).

We modeled the s_N of the 154 sites using environmental factors (Table S4). We then analyzed the s_N of N-limited and N-saturated forests and verified if there were significant differences on the global and biome scales. In Western Europe, North America, and East Asia, where there were abundant sites, we also compared the s_N of forests with N-limited or N-saturated status on a regional scale. The mean s_N was significantly different on global and regional scales (p <0.001; Fig. S9), proving that s_N can indicate N limitation or saturation status in forests.

Then we calculated an optimal threshold for s_N using data from 154 sites with field-observed N saturation status and s_N information. The bootstrap method accounted for the different sample sizes of N-limited and N-saturated sites (Davison & Hinkley, 1997). Specifically, from the 154 sites, we randomly sampled 10 N-limited and 10 N-saturated sites and selected a cutoff value for their s_N at a precision of 0.0001 kgN_2O-N kgN^{-1}. Sites in which s_N were above the cutoff value were classified as "N-saturated," and the rest were classified as "N-limited." The classified N saturation status of the sites was compared with field observations to determine the accuracy of the classification, which was calculated as the proportion of sites accurately classified into the same category as that observed. All possible cutoff values were tested, and the one with the highest classification accuracy was the "optimal" cutoff value. Random sampling and detection of optimal cutoff values were repeated 5000 times, during which some optimal cutoff values were detected more frequently than others. The optimal threshold for s_N in all samples was the most frequently detected optimal cutoff value, which was 0.0143 $kgN_2O\text{-}N\ kgN^{-1}$.

The N saturation status of global forests was determined based on the optimal threshold. Forests with s_N above the threshold were classified as N-saturated, and the rest were classified as N-limited. The accuracy of the classification was higher than 70% on global and regional scales (Fig. S6). Based on the classification, we produced a rasterized map of N-limited and N-saturated forests (0.5° × 0.5° resolution) in ArcGIS (ESRI, 2011).

Text S2. Inferring the variation of methane production and oxidation rates from the variation of observed methane fluxes

Soil CH_4 flux observed on the soil-air interface is codetermined by methane production (methanogenesis) and oxidation rates (Eq. S3). However, it has been difficult to disentangle the responses of methane production and oxidation to N input, because of the limited ability to separately observe methanogenesis and methane oxidation processes in the field. Here, we inferred the variation of methane production and oxidation rates from the variation of observed methane fluxes. This could further support the "three stage" hypothesis we proposed.

$$R_{CH4} = R_{CH4\_prod} - R_{CH4\_oxid} \quad \text{(Eq. S3)}$$

where R_{CH4} is the observed soil CH_4 flux (kg ha^{-1} yr^{-1}), positive R_{CH4} value means methane emission, whereas negative R_{CH4} value means methane uptake; R_{CH4_prod} is methane production rate (kg ha^{-1} yr^{-1}); R_{CH4_oxid} is methane oxidation rate (kg ha^{-1} yr^{-1}).

The change in methane production and oxidation rates could hardly be inversely calculated from the R_{CH4} values. Here, we inferred the change in R_{CH4_prod} and R_{CH4_oxid} by analyzing the mean values and standard deviations of R_{CH4}.

Firstly, the standard deviation of R_{CH4} could be calculated from that of R_{CH4_prod} and R_{CH4_oxid} (not considering the interaction between R_{CH4_prod} and R_{CH4_oxid}; Eq. S4).

$$SD(R_{CH4}) = \sqrt{SD(R_{CH4\_prod})^2 + SD(R_{CH4\_oxid})^2} \quad \text{(Eq. S4)}$$

Usually, when the expected value of a variable becomes higher, its observations will be more dispersed. This is because the random errors in the observations are often proportional to their values. That is to say, statistical dispersion of R_{CH4_prod} and R_{CH4_oxid} (as indicated by their standard deviations) should be positively related to their mean values.

Therefore, the decrease in the standard deviation of R_{CH4} under high N input (Fig. S2) may result from: (1) R_{CH4_prod} decreased under high N input, and R_{CH4_oxid} didn't change or slightly increased; (2) R_{CH4_oxid} decreased under high N input, and R_{CH4_prod} didn't change or slightly increased; (3) both R_{CH4_prod} and R_{CH4_oxid} decreased under high N input.

Meanwhile, we observed that the mean values of R_{CH4} remained nearly unchanged under high N input (Fig. S1a), which may result from: (i) both R_{CH4_prod} and R_{CH4_oxid} increased under high N input; (ii) both R_{CH4_prod} and R_{CH4_oxid} decreased under high N input; (iii) both R_{CH4_prod} and R_{CH4-_oxid} remained constant under high N input.

Combining the two evidences (standard deviation and mean values of R_{CH4} under high N input), it can be inferred that only hypotheses (3) and (ii) can be true at the same time. That is, both R_{CH4_prod} and R_{CH4_oxid} decreased under high N input.

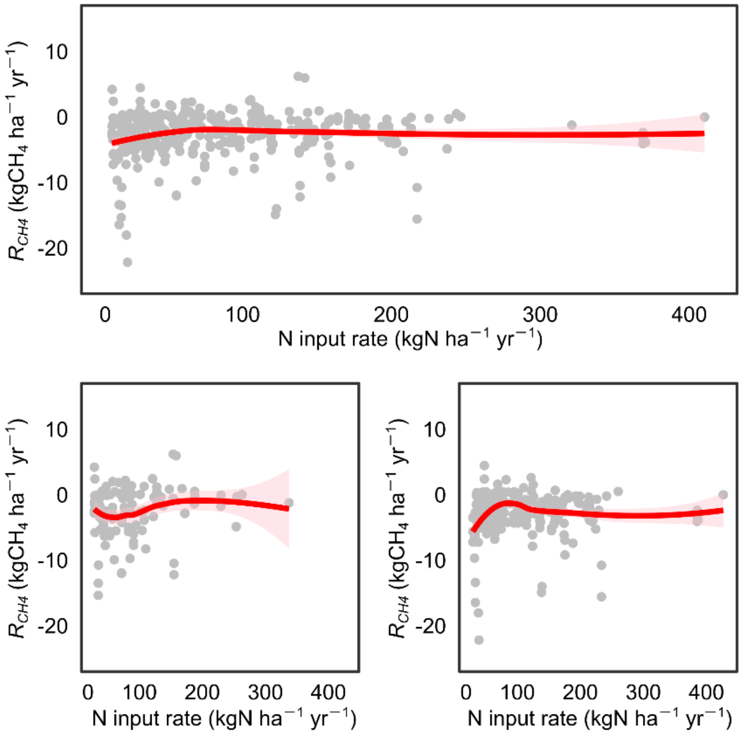

Fig. S1. Locally weighed regression ("LOWESS") model on soil CH_4 emission rate and N input rate. (a) Using all observations compiled from global N addition experiments, the N input rates of which were no greater than 400 kgN ha^{-1} yr^{-1} (n = 448). The few but variable observations on soil CH_4 fluxes at sites where N input rates were above 400 kgN ha^{-1} yr^{-1} (n = 17) were not used in further analysis. (b) LOWESS model constructed using data from N-limited sites and also where N addition experiments have been conducted for no more than 3 years when CH_4 emissions were observed (n = 131); (c) LOWESS model constructed using data from N-saturated forests, or data from sites where N addition experiments have been conducted for more than 3 years before observing the CH_4 fluxes (n = 317). Pink shadings represent the standard errors of the fitted models.

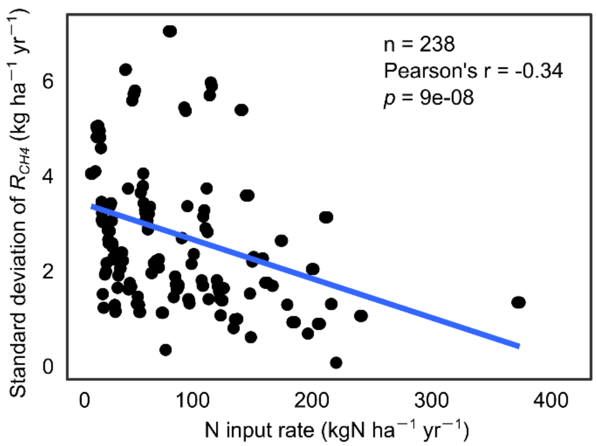

Fig. S2. Standard deviation of soil methane flux (R_{CH4}) was negatively correlated to N input rate. Data corresponding to N input levels above 400 kgN ha^{-1} yr^{-1} were not included in this analysis, because the very limited observations may not sufficiently reveal the statistical distribution of R_{CH4}. There were 238 unique N input rates that was no greater than 400 kgN ha^{-1} yr^{-1}. In practice, standard deviation was calculated for R_{CH4} corresponding to each N input rate, and N input rates less than 2 kgN ha^{-1} yr^{-1} in difference (e.g., standard deviation of R_{CH4} corresponding to 5 kgN ha^{-1} yr^{-1} was calculated using observations whose N input rates were within the range of 3 to 7 kgN ha^{-1} yr^{-1}). That was to make sure that there were sufficient observations for each N input level.

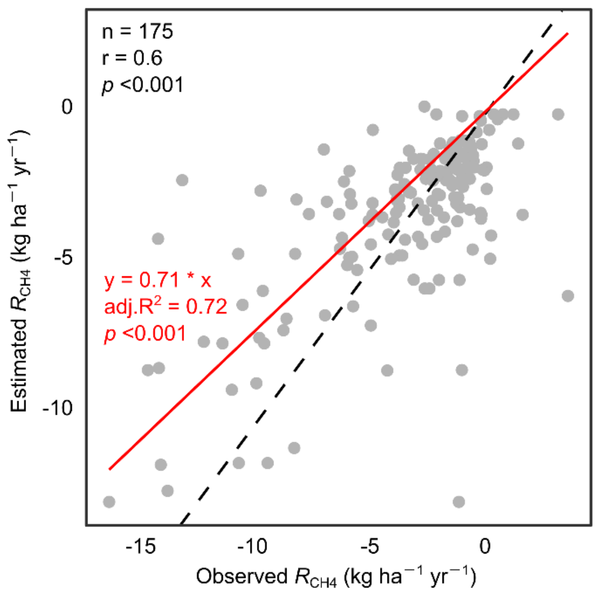

Fig. S3. Comparing observed soil CH_4 flux (R_{CH4}) in testing dataset with that estimated using averaged outputs from 1,000 random forest regression models. The red line and font indicate the fitted linear model on estimated and observed R_{CH4} values.

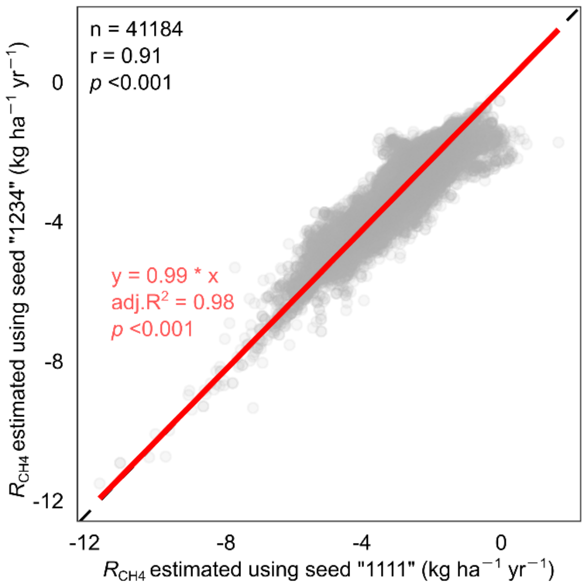

Fig. S4. Comparing soil CH_4 flux (R_{CH4}) estimated from different models built out of different training datasets. The sampling of observations to form a training (or testing) dataset was randomized by using different "seeds". Each seed corresponds to a determined set of samples, and different seeds lead to different samples. In this study, we randomly used seeds "1111" and "1234" for sampling. This analysis was to ensure that the estimated R_{CH4} values were not dependent on which data were used for training and testing the models, so that the derived spatial pattern of R_{CH4} was robust on grid level.

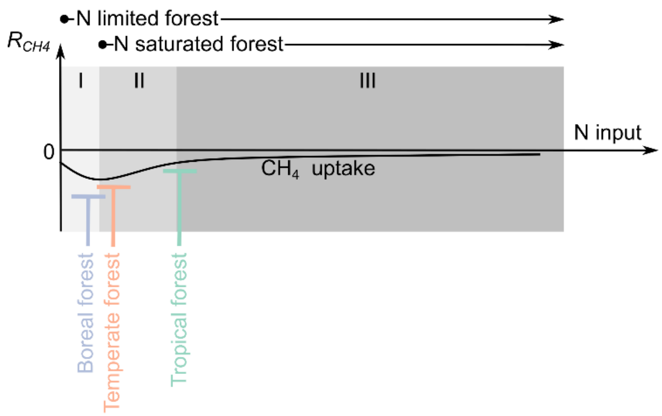

Fig. S5. Various forests are at different “stages” (in the stimulating-suppressing-weakening “three stages” framework), in accordance with the overall effects of N deposition on soil CH_4 fluxes in the forests.

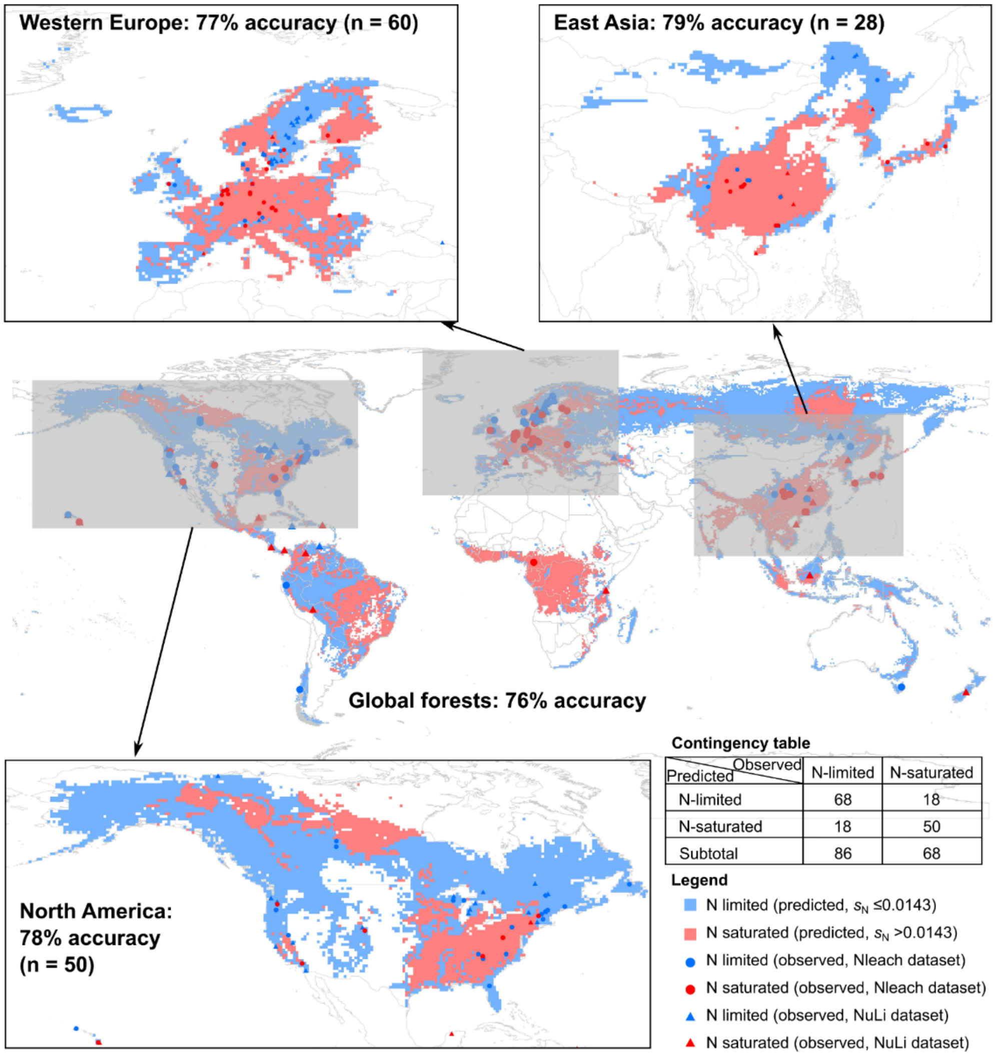

Fig. S6. Classified N-limited and N-saturated forests based on the sensitivity of soil N_2O emission to N deposition (s_N) compared with field-observed N limitation or saturation status, with extra details in regions where field-observations were more abundant.

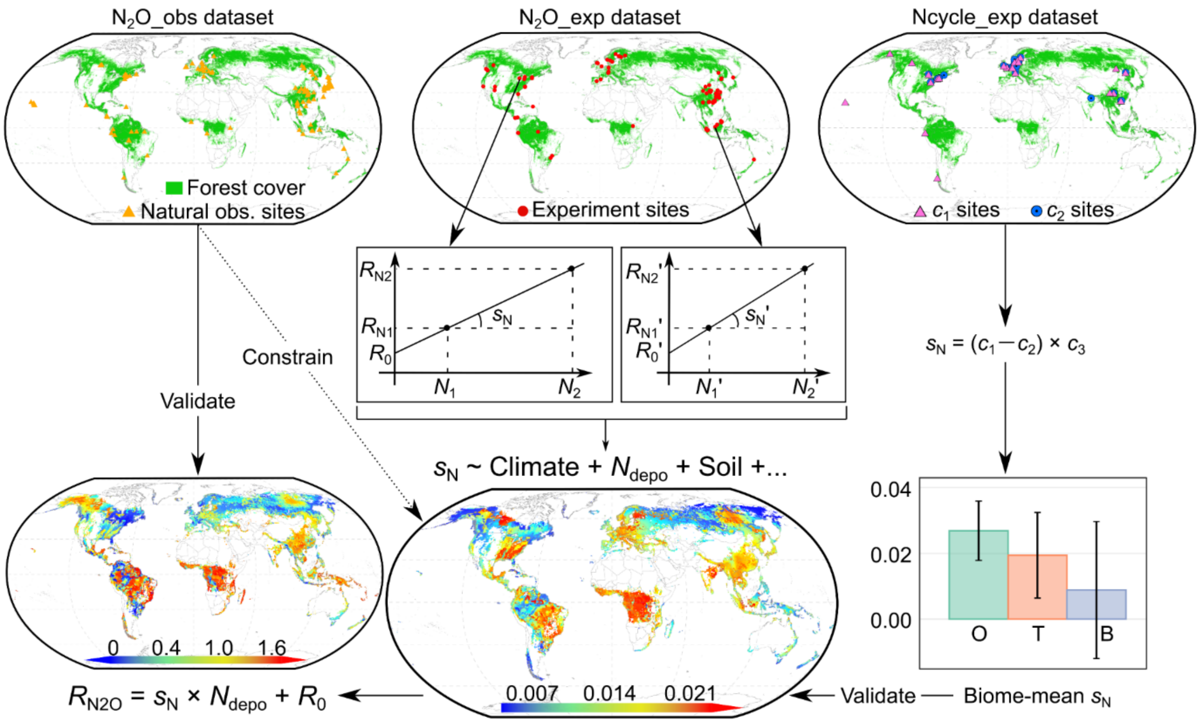

Fig. S7. Workflow illustrating the quantification and validation of the sensitivity of soil N_2O emission to N deposition (s_N) of global forests. N_1 and N_2 are different rates of low N input, and R_{N1} and R_{N2} are the corresponding soil N_2O emission rates. N_{depo}: N deposition rate (kgN ha^{-1} yr^{-1}); R_0: background soil N_2O emission rate (kgN_2O-N ha^{-1} yr^{-1}); c_1: sensitivity of N loss to N deposition (kgN kgN^{-1}); c_2: sensitivity of N leaching to N deposition (kgN kgN^{-1}); c_3: ratio of N_2O to other gaseous end-products from nitrification and denitrification processes (kgN_2O-N kgN^{-1}). O: Tropical; T: Temperate; B: Boreal.

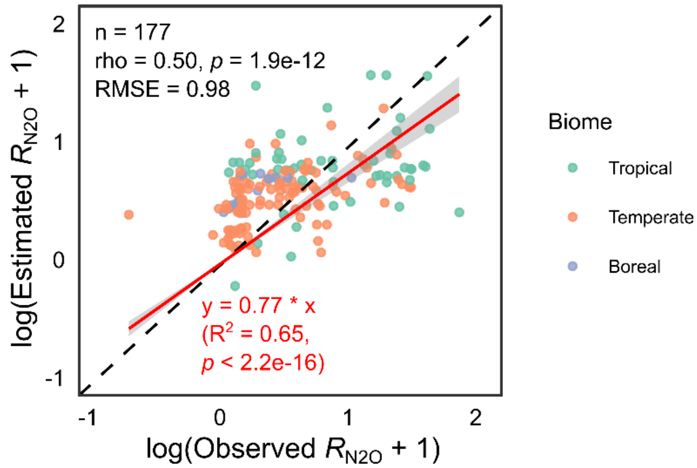

Fig. S8. Comparing estimated and observed soil N_2O emission rates (R_{N2O}). Observations were aggregated to 0.5°×0.5° grids to match with the spatial resolution of the environmental factors. Each point represents a grid-year. Points of different colors represent grid-years in different biomes. Dashed black line is the 1:1 line. The red line and fonts show a linear regression model on estimated and observed R_{N2O}.

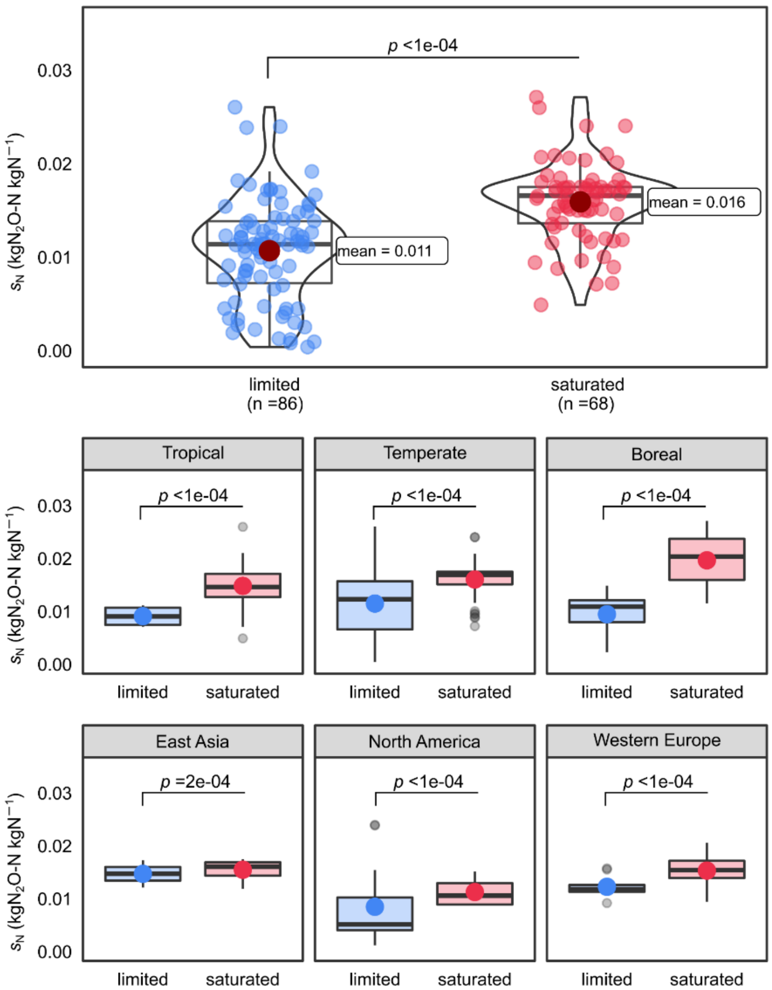

Fig. S9. Comparing the sensitivity of soil N_2O emission to N deposition (s_N) of N-limited and N-saturated forests on global and regional scales.

Table S1. Parameters of segmented linear regression models on soil CH_4 flux (R_{CH4}) and N input rate.

No.	Model (R_{CH4} ~ N input rate)	Parameters
①	y = -0.037*x – 2.45	n = 53, R^2 = 0.01, p = 0.44
②	y = 0.045*x – 5.75	n = 49, R^2 = 0.06, p = 0.09
③	y = -0.004*x – 0.73	n = 29, R^2 = 0.00, p = 0.80
④	y = 0.096*x – 5.28	n = 121, R^2 = 0.10, p = 0.0003
⑤	y = -0.006*x – 1.53	n = 196, R^2 = 0.03, p = 0.02

Table S2. Parameters of the constructed random forest regression models.

Model	R_{CH4} ~ MAT + MAT.cv + MAP + MAP.cv + N_{depo} + N_{depo}.cv + Sand + Clay + s_N	
	mtry	3
Parameters	ntree	1000
	Number of runs	1000

R_{CH4}: soil CH_4 emission rate; MAT: mean annual temperature; MAP: mean annual precipitation; N_{depo}: mean annual N deposition; Sand: soil sand content; Clay: soil Clay content; MAT.cv, MAP.cv and N_{depo}.cv are the corresponding coefficients of temporal variation; s_N: sensitivity of soil N_2O emission to N deposition, which indicates soil N limitation or saturation status. The predictors were selected based on mechanistic relevance and data availability.

Table S3. Linear models on soil N_2O emission rate (R_{N2O}) and N input rate (model: R_{N2O} ~ N input rate) built with low N input data (N addition rate ≤ 150 kgN ha^{-1} yr^{-1}) from global forest experiment sites, and the derived sensitivity (s_N) of soil N_2O emission to N deposition and background N_2O emission rate (R_0).

No.	Longitude range	Latitude range	Biome	s_N	R_0	n	adj.R^2	p value	References
1	(19,19.5)	(64,64.5)	Boreal	0.002	0.045	2	NA	NA	(Rutting et al., 2021)
2	(30.5,31)	(62.5,63)	Boreal	0.025	5.132	4	0.14	0.347	(Regina et al., 1998)
3	(22.5,23)	(62,62.5)	Boreal	0.013	0.538	2	NA	NA	(Ojanen et al., 2019)
4	(8,8.5)	(58.5,59)	Boreal	0.026	0.343	6	0.57	0.052	(Sitaula et al., 1995a, 1995b)
5	(-3.5,-3)	(55.5,56)	Temperate	0.02	0.258	6	0.18	0.224	(U. M. Skiba et al., 1998)
6	(-3,-2.5)	(55.5,56)	Temperate	0.006*	-0.009	6	0.73	0.019	(U. Skiba et al., 1999; U. M. Skiba et al., 1998)
7	(1.5,2)	(52.5,53)	Temperate	0.004	0.233	2	NA	NA	(U. M. Skiba et al., 1998)
8	(9.5,10)	(51.5,52)	Temperate	0.042*	0.51	10	0.48	0.015	(Borken et al., 2002; Brumme & Beese, 1992; Marife D Corre et al., 2003)
9	(128.5,129)	(47,47.5)	Boreal	0.015	0.777	11	0.02	0.300	(He, 2015; L. Song et al., 2017; Tian et al., 2018)
10	(8.5,9)	(47,47.5)	Temperate	0.003	-0.062	4	0.63	0.134	(Krause et al., 2013)
11	(-80.5,-80)	(43.5,44)	Temperate	0.009	1.374*	4	0.79	0.073	(Lutes et al., 2016)
12	(-72.5,-72)	(43,43.5)	Temperate	0.012	-0.216	2	NA	NA	(M. S. Castro et al., 1992)
13	(141,141.5)	(43,43.5)	Temperate	0.025	1.647	2	NA	NA	(Y. S. Kim et al., 2012)
14	(-72.5,-72)	(42.5,43)	Temperate	0.001	0.074	6	0.05	0.323	(Richard D. Bowden et al., 1991)
15	(128,128.5)	(42,42.5)	Temperate	0.01	0.67	2	NA	NA	(Geng et al., 2017)
16	(127.5,128)	(41.5,42)	Temperate	0.029	2.287	13	0.11	0.141	(Bai et al., 2014; Cheng et al., 2016; B. Peng et al., 2021)
17	(-80.5,-80)	(41.5,42)	Temperate	0.003	0.217	2	NA	NA	(R. D. Bowden et al., 2000)
18	(-4,-3.5)	(40,40.5)	Temperate	0.001*	0.026*	4	0.95	0.017	(Lafuente et al., 2020)
19	(112,112.5)	(36.5,37)	Temperate	0.056	2.754	3	0.98	0.068	(H. Yu, 2019)
20	(111,111.5)	(31.5,32)	Temperate	0.013**	0.483	27	0.28	0.003	(Zhaolan Lin, 2013; Zhaolan Lin et al., 2012; R. Wang, 2012; Xu et al., 2017)
21	(110,110.5)	(31.5,32)	Temperate	0.023	-0.31	4	0.54	0.166	(Pan, 2013)
22	(120.5,121)	(30.5,31)	Temperate	0.017	1.135	4	0.51	0.181	(Tu & Zhang, 2018)
23	(119.5,120)	(30,30.5)	Temperate	0.003	1.238***	16	0.01	0.308	(X. Chen, 2014; X. Chen et al., 2014; Ziwen Lin, 2019; X. Z. Song et al., 2020; Z. Wang, 2014)
24	(120,120.5)	(30,30.5)	Temperate	0.012**	0.834*	12	0.64	0.001	(J. Zhang, 2013; J. Zhang et al., 2013)
25	(106.5,107)	(29.5,30)	Temperate	0.025*	0.875*	3	1	0.018	(Xie et al., 2018)

26	(115.5,116)	(29.5,30)	Temperate	0.012	2.025	6	0.14	0.248	(C. Li et al., 2019)
27	(116.5,117)	(28,28.5)	Temperate	0.013	0.16	2	NA	NA	(Fan et al., 2020)
28	(118,118.5)	(27,27.5)	Tropical	0.015	1.948	9	0.12	0.190	(S. Chen, 2012)
29	(115,115.5)	(26.5,27)	Tropical	0.026***	-0.092	54	0.47	<0.001	(Dang, 2015; X. Li, 2017; X. Y. Li et al., 2015; Sun & Zhang, 2015; J. Wang, 2016; L. Wang, 2015; L. Wang et al., 2016; Y. Wang, 2015; Y. S. Wang et al., 2016; L. Zhang, 2013)
30	(117,117.5)	(26,26.5)	Tropical	0.007	0.5	3	0.55	0.313	(Wu, 2018)
31	(118,118.5)	(25.5,26)	Tropical	0.012	0.601	4	0.33	0.257	(Yuan, 2016)
32	(113,113.5)	(23.5,24)	Tropical	0.014	-0.226	3	0.77	0.220	(Cai, 2013)
33	(112.5,113)	(23,23.5)	Tropical	0.027*	0.19	22	0.15	0.041	(H. Chen et al., 2016; Gao et al., 2017; Mo et al., 2006)
34	(112.5,113)	(22.5,23)	Tropical	0.004	1.919***	14	0.11	0.129	(W. Zhang et al., 2014)
35	(106.5,107)	(22,22.5)	Tropical	0.012***	-0.038	8	0.84	0.001	(Hong, 2015)
36	(107,107.5)	(22,22.5)	Tropical	0.043*	-0.089	10	0.51	0.013	(R. Li et al., 2014, 2015; Yang, 2015; Kai Zhang et al., 2015)
37	(107.5,108)	(22,22.5)	Tropical	0.007**	0.589**	4	0.98	0.007	(K. Zhang et al., 2017)
38	(101,101.5)	(21.5,22)	Tropical	0.037	2.101*	9	0.18	0.144	(Yan, 2006; Zhou et al., 2016)
39	(110.5,111)	(21,21.5)	Tropical	0.018	3.195	3	0.69	0.256	(F. M. Wang et al., 2014)
40	(-80,-79.5)	(9,9.5)	Tropical	0.021**	0.674	8	0.71	0.005	(M. D. Corre et al., 2014; Koehler et al., 2009)
41	(-82.5,-82)	(8.5,9)	Tropical	0.019	1.063	8	0.32	0.083	(M. D. Corre et al., 2014; Koehler et al., 2009)
42	(116.5,117)	(6,6.5)	Tropical	0.007**	0.517**	10	0.61	0.005	(Hall et al., 2004)
43	(31.5,32)	(1.5,2)	Tropical	0.018***	1.756***	4	1	0.001	(Tamale et al., 2021)
44	(102,102.5)	(-1.5,-1)	Tropical	0.022**	0.919*	7	0.84	0.002	(Aini et al., 2015)
45	(-79.5,-79)	(-4,-3.5)	Tropical	0.005	0.135	3	0.44	0.356	(Muller et al., 2015)
46	(-79,-78.5)	(-4.5,-4)	Tropical	0.006	0.471	3	0.5	0.333	(Muller et al., 2015)
47	(-79.5,-79)	(-4.5,-4)	Tropical	0.006	-0.11	3	0.95	0.106	(Muller et al., 2015)

* p <0.05; ** p <0.01; *** p <0.001; NA, not applicable

Table S4. Generalized linear models on environmental factors and the sensitivity (s_N) of soil N_2O emission to N deposition and the background N_2O emission rate (R_0).

	Estimate	SE	t	*p*
Refined model on s_N† (Deviance explained = 91.1%, n=46)				
Clay	4.77E-03	1.83E-03	2.605	0.013*
Sand	3.15E-03	9.20E-04	3.419	0.001**
log(N_{depo})	2.01E-02	1.14E-02	1.769	0.085
Clay × log(N_{depo}.cv)	2.13E-03	9.35E-04	2.282	0.028*
Sand × log(N_{depo}.cv)	1.17E-03	3.82E-04	3.056	0.004**
Clay × Sand	-1.90E-04	6.94E-05	-2.735	0.009**
Clay × Sand × log(N_{depo}.cv)	-1.14E-04	3.66E-05	-3.112	0.003**
Refined model on R_0‡ (Deviance explained = 43.2%, n = 45)				
log(N_{depo}.cv)	1.99E-01	9.56E-02	2.084	0.043*
MAT × Sand × Clay	3.04E-06	5.99E-07	5.072	0.000***
MAP × MAP.cv × log(N_{depo})	-8.31E-04	2.91E-04	-2.854	0.007**

MAT: mean annual temperature; MAP: mean annual precipitation; N_{depo}: mean annual N deposition; Sand: soil sand content; Clay: soil clay content.

† s_N ~ (Clay + Sand + log(N_{depo}) + Clay × log(N_{depo}.cv) + Sand × log(N_{depo}.cv) + Clay × Sand + Clay × Sand × log(N_{depo}.cv))^2

‡ R_0 ~ EXP(log(N_{depo}.cv) + MAT × Sand × Clay + MAP × MAP.cv × log(N_{depo})) – 0.5

* p <0.05; ** p <0.01; *** p <0.001

Data Set S1. (separate file)
Compiled dataset on soil CH_4 flux from N addition experiments in global forests (CH_4_exp dataset in main text).

Data Set S2. (separate file)
Compiled data on soil CH_4 flux under natural conditions in global forests (CH_4_obs dataset in main text).

Data Set S3. (separate file)
Compiled dataset on soil N_2O emission rate from N addition experiments in global forests (N_2O_exp dataset in Text S1).

Data Set S4. (separate file)
Compiled data on soil N_2O emission rate under natural conditions in global forests (N_2O_obs dataset in Text S1).

Data Set S5. (separate file)
Compiled dataset on N loss rate, N leaching rate and change rate of soil N pool from N addition experiments in global forests (Ncycle_exp dataset in Text S1).

Data Set S6. (separate file)
Compiled dataset on global forest N saturation status (limited or saturated) indicated by N leaching rate (Nleach dataset in Text S1).

Data Set S7. (separate file)
An existing dataset from Du et al. (2020) on global forest N saturation status (limited or saturated) indicated by plant growth response to N input (NuLi dataset in Text S1).

Data Set S8. (separate file)
Data on environmental factors (MAT, MAP, N deposition rate, etc.) in global forests, extracted from spatial datasets mentioned in Methods section.

Data Set S9. (separate file)
Global forest soil methane budgets estimated in previous studies.

Code S1. (separate file)
R code script used to carry out the data analysis processes, and produce the figures.